基于微观损伤机理的延性裂纹扩展行为分析

朱智军， 荆洪阳， 徐连勇， 霍立兴
（天津大学 材料科学与工程学院，天津 300072）

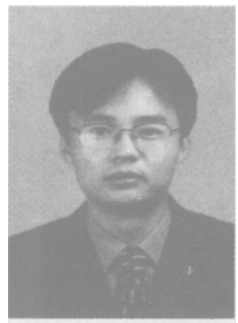

朱智军

摘 要：在考虑材料内部塑性损伤的基础上，通过有限元数值方法（特殊单元模型法），编制了求解韧性断裂特征参量的程序，模拟材料的韧性断裂过程。通过单轴拉伸试验的模拟结果，得出反映材料微观损伤的控制参量，再根据该参量对同种材料的标准三点弯曲试验进行定量预测，即实现从一种试验结果预测同种材料的其它试验结果。结果表明，在韧性裂纹扩展时，考虑塑性损伤的特殊单元模型能够很好地描述材料的韧性断裂过程，可以实现同种材料不同试验间相互预测的目的。

关键词：塑性损伤；有限元数值方法；试验；韧性断裂
中图分类号：TH404 文献标识码：A 文章编号：0253－360X(2006)08－067－04

0 序 言

在钢铁结构中，一些关键结构（如大型建筑物、航海设施、核设施、石油和天然气管道等）经常发生变形，使得材料韧度和强度降低，导致结构断裂，材料的安全可靠性问题引起人们的极大关注。另一方面，为了使焊接钢结构最大限度地发挥材料的潜能，即使产生延性裂纹，只要不发生失稳扩展就允许使用，可以节省大量资金或人力物力。因此对于韧性断裂的研究不仅具有理论价值，还具有其潜在的巨大的经济效益[1~4]。国内外许多专家从力学、冶金学等许多方面对韧性材料的塑性变形以及韧性断裂进行了广泛和深入研究，提出了多种模型。目前应用最广泛的、理论较为完善的韧性断裂模型是 Gurson-Tvergaard 的多孔微观机制模型（G－T 模型）[5]，该模型定量描述了塑性变形量和空穴形核、长大及扩展的关系。Xia 和 Shih 在 G－T 模型的基础上，基于空穴扩张的材料微观塑性损伤提出了特殊单元模型[6,7]。

目前，国内应用此种模型对试验（拉伸试验和三点弯曲试验）的模拟分析至今未见报道。为此，提出基于特殊单元模型研究对同种材料不同试验进行相互预测。首先，对圆棒拉伸试验进行数值模拟分析，然后把几组数值结果与相应试验数据对比，验证其中一组数据的正确性，得到反映材料微观塑性损伤的控制参量（特殊单元尺寸 D_0 以及与之相应的空穴初始体积率 f_0、空穴临界体积率 f_c），根据该参量再对同种材料的标准三点弯曲试件数值分析，验证其正确性，为正确进行实际结构缺陷评定提供一定依据。同时当试验操作难度过大时，有限元数值模拟可以一定程度地代替试验。

收稿日期：2005－05－30
基金项目：国家自然科学基金资助项目（50275107）

1 试 验

试验中的 X65 管线钢（由海洋石油工程股份有限公司提供）采用低碳当量（低碳）、锰－铌微合金化、低硫以及加入稀土金属使硫化物变性（见表 1），从根本上保证了该钢具有各种优良的性能。对 X65 管线钢，根据标准制备圆棒拉伸和三点弯曲试样，试件尺寸如图 1 所示。

表 1 X65 钢管化学成分（质量分数，%）

Table 1 Chemical components of X65 pipe steel

C	Mn	Si	P	Ni	S	Nb	V
0.1	0.32	0.24	0.016	0.2	0.004	0.04	0.06

首先对圆棒拉伸试样进行了静载下的拉伸试验，获得该材料的力学性能（见表 2），为后面的数值计算提供对比依据。再对三点弯曲试样进行试验，其裂纹尖端张开位移（CTOD）值按英国标准 BS7448 计算。

图 2 给出了三点弯曲试样的阻力曲线，确定了试样延性裂纹启裂时的断裂韧度。这样试验数据就为后面的数值计算提供对比依据。

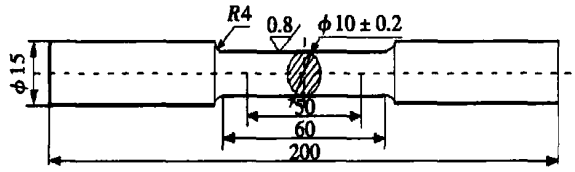

(a) 圆棒拉伸试样

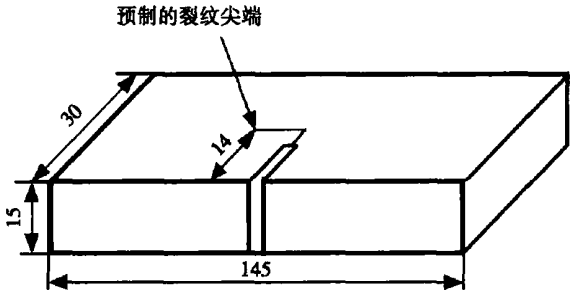

(b) 三点弯曲试样

图 1 试样几何形式 (mm)

Fig. 1 Specimen configuration

表 2 X65 管线钢力学性能

Table 2 Mechanical properties of X65 pipe steel

试样编号	截面直径 d_0(mm)	屈服强度 R_{eL}/MPa	抗拉强度 R_m/MPa	强度比 R_{eL}/R_m	断后伸长率 A(%)	断面收缩率 Z(%)
1	10.00	547.493	658.901	0.831	27.8	78.1
2	10.02	534.098	630.286	0.847	27.0	77.6
3	10.01	537.388	635.981	0.845	27.2	78.5
平均值		539.660	641.723	0.8411	27.333	78.07

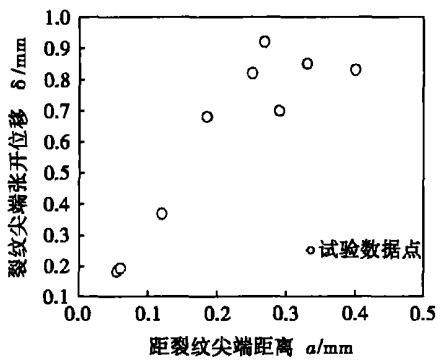

图 2 R 曲线测试结果

Fig. 2 Tested results of R-curve

2 特殊单元模型理论

采用有限元数值方法, 分析研究延性裂纹扩展行为, 建立特殊单元模型, 进而模拟延性裂纹扩展。

早期 Gurson-Tvergaard 模型[5] 关系决定了裂纹前端区域内空穴扩张和由于空穴增长带来的材料宏观软化, 并提出了下面的屈服函数式。

$$\Phi=\left(\frac{\sigma_{eq}}{\sigma_0}\right)+2q_1 f\cosh\left(\frac{3}{2}\frac{q_2\sigma_m}{\sigma_0}\right)-(1+q_3 f^2)=0, \quad (1)$$

式中: σ_{eq}表示 Mises 等效应力; σ_m 表示宏观静水压力; σ_0 表示特殊单元中母材的流变应力; f 代表空穴的体积比, 当 $f=0$ 时, 则表示均质、不可压缩材料的 Mises 屈服表面; 在多轴应力状态下 $\sigma_{eq}=(3S_{ij}S_{ij}/2)^{1/2}$, 其中 S_{ij}代表 Cauchy 应力偏量; q_1, q_2, q_3 是由 Tvergaard 提出的系数, $q_1=1.5$, $q_2=1.0$, $q_3=q_1^2$。当 $q_1=q_2=q_3=1$ 时, 就是 Gurson 模型的最初表达式。

Xia 和 Shih 在 G-T 模型的基础上, 基于空穴扩张的材料微观塑性损伤提出了特殊单元模型[6,7]。图 3 为该模型的示意图。空穴扩张仅限于裂纹尖端宽度为 D_0 的长条区域内, D_0 表征材料内部夹杂物之间的距离。在数值模拟计算中, 该区域是由含有初始空穴体积含有率 f_0(初始空穴体积与特殊单元体积之比)的特殊单元组成。

根据塑性力学理论, 如果空穴体积含有率 $f\ll 1$, 则空穴体积含有率增长率 $\dot{f}$可表示为

$$\dot{f}\approx\frac{3}{2}f\sinh\left(\frac{3}{2}\frac{\sigma_m}{\sigma_{eq}}\right)\dot{\varepsilon}_p, \quad (2)$$

式中: $\dot{\varepsilon}_p$ 为等效应变速率。

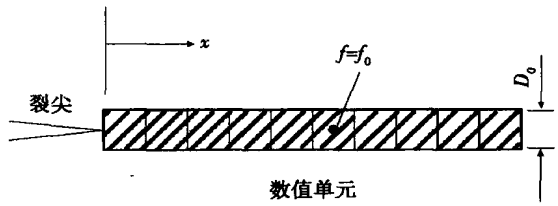

图 3 基于 Gurson 理论的特殊单元模型

Fig. 3 Cell model based on Gurson theory

对式(2)分析后, 可知特殊单元尺寸 D_0、初始空穴体积含有率 f_0 和临界空穴体积含有率 f_c 是控制延性裂纹扩展的基本参量。根据 Shih[6,7] 等的研究结果, 在数值模拟计算中, 若将延性裂纹启裂时的 CTOD 值(由试验的阻力曲线确定)作为特殊单元宽度 D_0, 计算结果和试验结果非常吻合; 而对于初始空穴体积含有率 f_0 和临界空穴含有率 f_c, 则由如下方法确定: 采用一系列的 f_0 和 f_c(试验表明 f_c 的影响并不是很显著), 分别对拉伸试件进行数值计算, 把计算数据结果(几组载荷—位移曲线)与试验对比, 如果计算的某一条载荷—位移曲线与试验结果相符, 则该条阻力曲线的 f_0 和 f_c 参量为材料本身所具有的特性, 可以实现从一种试验结果预测同种材料的其它试验结果[8]。

3　三点弯曲试样和圆棒拉伸试样有限元计算及对比分析

为分析研究三点弯曲试验和拉伸试验之间的相互预测，首先采用有限元数值方法对试验进行模拟。

图 4 为所采用三维有限元数值计算单元划分图，用于有限元计算的圆棒拉伸试样和三点弯曲试样，由于其呈对称性，取试样的 1/4 建模。为消除单元划分对结果的影响，与试件形式无关，裂纹尖端采用相同的单元形式，最小单元尺寸为 0.1 mm×0.1 mm×0.1 mm，后处理的计算程序为 WARP3D。采用裂纹尖端张开位移表征裂纹尖端的载荷水平，计算方法和试验中所采用方法相同。

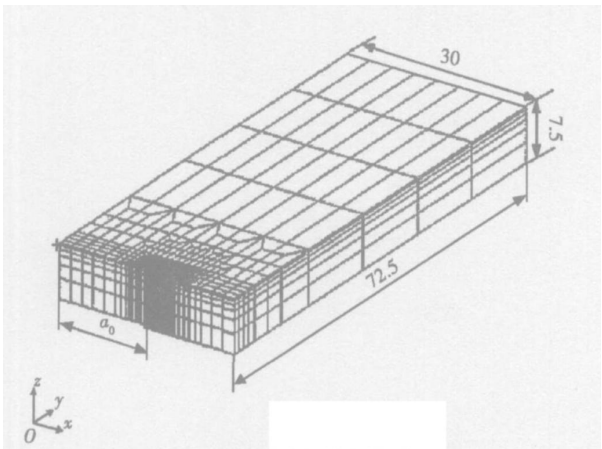

(a) 三点弯有限元模型

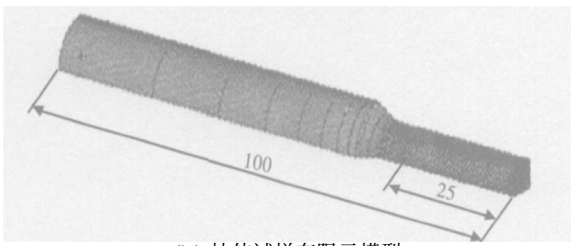

(b) 拉伸试样有限元模型

图 4　有限元计算单元划分（mm）

Fig. 4　Finite element models

对拉伸试件，由有限元数值分析得出的一系列载荷—位移曲线，其中有一组数据与试验所得的载荷—位移曲线基本符合，如图 5 所示。从而得到与特殊单元尺寸 D_0 相对应的空穴的初始体积含有率 f_0，并将这组值作为反映材料塑性损伤的特殊单元模型控制参量，即 $D_0=0.2$ mm，$f_0=0.0035$，$f_c=0.2$。

在拉伸试件有限元数值模拟中，已经确定了与 X65 钢对应的反映材料塑性损伤的特殊单元模型控制参量 $D_0=0.2$ mm，$f_0=0.0035$，$f_c=0.2$，在此基础上，再用WARP3D软件对拉伸模型进行后处理

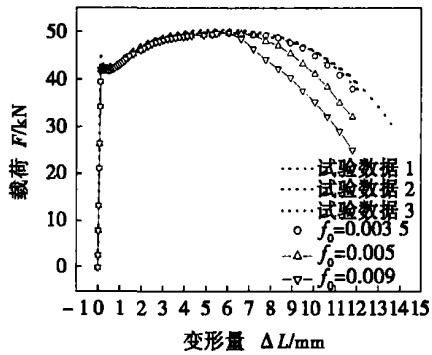

图 5　拉伸试样的有限元模拟与试验位移—载荷曲线

Fig. 5　Tensile specimen FEM and tesed displacement-load curves

计算，将数据结果整理并与试验结果的阻力曲线相对比，如图 6 所示。从图中可以看出，根据反映材料塑性损伤的特殊单元模型控制参量 $D_0=0.2$ mm，$f_0=0.0035$，$f_c=0.2$，对三点弯曲试验进行了定量预测，尤其是对载荷下降段的塑性变形过程的模拟，其计算结果与试验结果相当吻合。

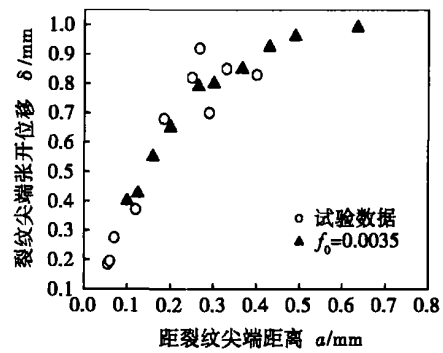

图 6　三点弯模拟结果与试验的阻力曲线

Fig. 6　Simulated results of 3-point bend and tested R-curves

4　结　　论

（1）根据延性裂纹微观机理，采用特殊单元模型，利用有限元数值方法得到单轴拉伸试验载荷—位移曲线（共有 3 条），并与试验结果比较，得出了反映材料微观损伤的控制参量，再根据该参量对同种材料的标准三点弯曲试样进行了预测。

（2）在韧性裂纹扩展时考虑塑性损伤的特殊单元模型能够很好地描述材料的韧性断裂过程，并能实现同种材料不同试验间的相互预测。

参考文献：

[1]　Claudio Ruggieri, Fernando F Santos, Mitsuru Ohata, *et al*. Cell

model prediction of ductile crack initiation in damaged pipelines[J]. Proceedings of the International Pipe Dreammer's Conference, 2002, 26(3): 917—929.

[2] Gao X, Faleskog J, Shih C F, *et al*. Ductile tearing in part-through crack: experiments and cell-model predictions[J]. J. Mech. Phys, 1998, 46(6): 761—777.

[3] Rice R J, Tracey D M. On the ductile enlargement of voids in triaxial stress fields[J]. J. Mech. Phys. Solids, 1969, 17(3): 201—217.

[4] McMeeking R M. Finite deformation analysis of crack-tip opening in elastic-plastic materials and implications for fracture[J]. J. Mech. Phys. Solids, 1977, 25(5): 357—381.

[5] Tvergaard V. Materials failure by void growth to coalescence[J]. Advances in Applied Mechanics, 1990, 27(1): 83—151.

[6] Xia L, Shih C F. A numerical study using computation cells with micro-structureally based length scales[J]. J. Mech. Phys. Solids, 1995, 43(2): 233—258.

[7] Xia L, Shih C F. Void nucleation and geometry effects on macro-scopic fracture behavior[J]. J. Mech. Phys. Solids, 1996, 44(3): 603—639.

[8] 荆洪阳, 霍立兴, 张玉凤, 等. 基于微观损伤模型的强度非匀质焊接接头抗延性裂纹扩展阻力特性研究[J]. 机械强度, 2000, 22(3): 200—202.

作者简介：朱智军，男，1978 年 11 月出生，硕士研究生。研究方向为焊接结构强度与断裂，发表论文 1 篇。

Email：zzjun2005@eyou.com

ty, which makes the Young's modulus increase. If was found that the spraying orientation has effect on Young's modulus of coating which takes on the anisotropic property. In addition, interface fracture toughness was also introduced, which mainly include the 4-point bend test to measure interface critical strain energy rate, improved tensile test and local approach based on Weibull criterion.

Key words: coatings; Young's modulus; three-point bending; two-side coated specimen; interface fracture toughness

Analysis of plasma-MIG arc signal based on LabVIEW BAI Yan, GAO Hongming, Lu Hao, Shi Lei (State Key Lab of Advanced Welding Production Technology, Harbin Institute of Technology, Harbin 150001, China). p59—62

Abstract: The arc electrical signals were collected the data acquisition system in the plasma-MIG welding process, and the U-t、I-t、U-I diagrams analyzed with the Labview software were obtained. The difference of arc characteristic between plasma-MIG arc and MIG arc was studied and the effect of increase of MIG current on the electric signals of the Plasma-MIG arc was analyzed. The unstable arc electrical signals of Plasma-MIG were gathered and the result indicates that some contacts exist between inner arc and outer arc.

Key words: plasma-MIG; MIG; arc signal; LabVIEW

Mechanical properties of CO_2-laser and TIG aluminium alloy welded joint ZHOU Qinglin, QIAO Jisen, CHEN Jianhong, ZHU Liang(State Key Laboratory of Gansu Advanced Non-ferrous Metal Materials, Lanzhou University of Technology, Lanzhou 730050, China). p63—66

Abstract: The mechanical properties of Al-alloy 5A02 and its welded joint of CO_2 laser welding and TIG welding were studied. And rolling— orientation and rolling— uprightness orientation mechanical properties were measured. In addition, series load experiments were used to study properties of weld and base metal. This study considered that material anisotropy affects welded-joint mechanical properties, which is relate to each area materials mechanical properties of welded joint, will provide the theoretical bases for investigation of welded joint, as well as provide the local mechanical properties experimental data for crash simulation of Al-alloy automobile components.

Key words: CO_2 Laser welding; TIG welding; welded joint; anisotropy; curve fitting.

Extension of ductile fracture based on micro-plastic damage ZHU Zhijun, JING Hongyang, XU Lianyong, HUO Lixing(School of Materials Science and Engineering, Tianjin University, Tianjin 300072, China). p67—70

Abstract: Considering the inner micro plastic damage , using the finite element method (the computational cell model) and compiling the program to get parameters controlled ductile crack growth, the process of ductile fracture was simulated. The parameters to controll ductile crack growth were gotten from the simulating uniaxial tension test, which means that tests of the same material can be forecasted each other based the cell model. The results indicate that the prediction is in a good agreement with the experiment, and the cell model gives a good description of ductile crack growth. The prediction between different tests of the same material is reasonable.

Key words: plastic damage; finite element numerical simulation; experiment; ductile fracture

Analysis on high strength Al-Li alloy joints brazed in furnace ZHANG Ling, XUE Songbai, HAN Zongjie, HUANG Xiang (College of Materials Science and Technology, Nanjing University of Aeronautics and Astronautics, Nanjing 210016, China). p71—74

Abstract: High strength Al-Li alloy was brazed in furnace by using Ag-Al-Cu-Zn filler metal with CsF-AlF3 flux. The results show that under the condition of N_2 atmosphere, the tensile strength of butt joint is up to about 390 MPa with the strength factor of 0.89 and the shear strength of lap joint is up to about 380 MPa with the strength factor of 0.86, which all the strength factors are higher than those of fusion welding and brazed joints of high strength Al-Li alloy reported. The experimental results and theoretical analyses show that, effectively destroying and removing the complex oxide films on the surface of Al-Li alloy under the temperature of about 530℃ is the key factor to the brazing process and the protection of N_2 is an important way to improve mechanical properties of the braze metal.

Key words: high strength Al-Li alloy; furnace brazing; strength factor; fractograph

Methods of safe assessment for offshore pipeline LIU Mingliang, ZHANG Yufeng, HUO Lixing, DENG Caiyan(School of Material Science and Engineering, Tianjin University, Tianjin 30072, China). p75—78

Abstract: Given crack size and load, two methods of Structure Integrity Assessment Procedure(SINTAP) sponsored by the European Commission and BS910 were applied to assessment for welded joints of the API 5LX65 pipeline steel with surface flaw at the weld toe. The assessment was carried out according to Limit Load Solutions and the CTOD(Crack Tip Opening Displacement) test result. The failure lines of level 0 and level 1(level 1 and level 2 of BS7910) of the weld were derived from the tensile test results. The assessment showed that the assessment point is located within the failure line of analysis level 0 and level 1(level 1 and level 2 of BS7910). So welded joint of the pipeline is safe and the values obtained by using the two methods are very similar. Analysis of these two methods gives a help to use different methods for pipeline structure assessment. This study laid the foundation of choosing different methods of pipeline structure assessment.

Key words: offshore pipeline; stuctural integrity; failure assessment diagram